A PRESSURE FLUX-SPLIT TECHNIQUE FOR COMPUTATION OF INLET FLOW BEHAVIOUR

H.S. Pordal, P.K. Khosla and S.G. Rubin
University of Cincinnati
Cincinnati, Ohio 45221-0343

ABSTRACT

A method for calculating the flow field in aircraft engine inlets is presented. The phenomena of inlet unstart and restart inlet are investigated. Solutions of the Reduced Navier Stokes (RNS) equations are obtained with a time consistent direct sparse matrix solver that computes the transient flow field both internal and external to the inlet. Time varying shocks and time varying recirculation regions can be efficiently analyzed. The code is quite general and is suitable for the compution of flow for a wide variety of geometries and over a wide range of Mach and Reynolds numbers.

INTRODUCTION

At supersonic flight mach numbers the flow within an aircraft engine inlet is very complex. Oblique and normal shocks are present and viscous interactions can be quite significant. These effects are amplified by the presence of adverse pressure gradients, and shock-boundary layer interaction plays an important role in determining the flow behaviour. At supersonic flight conditions, the performance of the inlet/diffuser depends critically on the nature of the shock interaction and, in particular, on the location of the terminal shock. At off-design flight conditions, for a given diffuser geometry, a shock can move ahead of the cowling so that inlet unstart occurs. This causes a sharp reduction in mass flow and pressure recovery and an associated large increase in drag. The shock can be swallowed (engine restart) by increasing the throat area or by decreasing the back pressure. The performance of the inlet then returns to the design value. These complex flow phenomena cannot be accurately predicted with analytical techniques. Computational methods can provide a reasonable estimate of the critical flow phenomena. Toward this goal, the present authors have previously investigated inviscid and low Reynolds numbers flow in two dimensional and axisymmetric inlets (1,2,3).

The present study deals with an investigation of the flow characteristics in typical aircraft engine inlets at large Reynolds number. A two dimensional/ axisymmetric flow solver for inlet flow field studies has been developed. The governing equations are written in general non-orthogonal curvilinear coordinates and are discretized using a form of flux vector splitting (4). This procedure was formulated previously by Rubin and Khosla (4,5). The discretization procedure remains the same for viscous and inviscid, incompressible, subsonic, transonic and supersonic flows, see Rubin and Khosla (6-10), and has been extended for three dimensional (11), as well as unsteady flow (1,2,3,12,13) computations. A significant feature of this procedure is that it does not require the addition of explicit artificial viscosity. Numerical dissipation due to the accuracy of the discretization can be minimized on sufficiently fine grids, see Rubin and Himansu (14).

For unsteady flow computations, in order to capture the transient behaviour efficiently, a more robust and time consistent procedure has been developed. A direct sparse matrix solver (15,16) has been appropriately modified for coupled systems of equations and is applied herein. The choice of the direct solver is dictated by considerations of stability, robustness, accuracy and time consistency. For steady computations, the solution technique permits large time increments and has strong convergence properties; whereas, for transient flows, time consistency is maintained in an efficient manner. Implicit, time consistent procedures based on approximate factorization, e.g. ADI techniques, typically do not have strong convergence properties and may require added transient or steady state artificial viscosity (17). The sparse matrix direct solver, considered herein, retains the simplicity and robustness of the time marching procedure and, as in the steady-state global relaxation formulation, explicitly added artificial viscosity is not required. Moreover, for time dependent computations, the time step limitation for the direct solver is much less severe than that for other time marching procedures.

The flow in an inlet at large Reynolds number is inherently turbulent. A simple algebraic two layer eddy viscosity (Baldwin-Lomax) model is used herein for turbulent flow computations. Section 2 presents the governing equations. The boundary conditions and discretization are described in Sections 3 and 4, respectively. Section 5 deals with the solution procedure and the results are discussed in Section 6.

GOVERNING EQUATIONS

The RNS equations are obtained from the full NS equations by neglecting the viscous diffusion terms in an appropriate streamwise direction, as well as all viscous diffusion terms in the normal momentum and energy balances. In this context, the RNS system represents a composite of the Euler plus second-order boundary layer equations. The conservation form of the RNS equations are written in general non-orthogonal curvilinear co-ordinates (ξ,η), so that an arbitrary grid generation technique can be applied.

Continuity Equation:

$$(\rho gr)_\tau + (\rho grU)_\xi + (\rho grV)_\eta = 0. \tag{1a}$$

X Momentum Equation:

$$[\rho gr(UX_\xi + VX_\eta)]_\tau + (\rho grU^2X_\xi)_\xi + (\rho grUVX_\eta)_\xi + (\rho grUVX_\xi)_\eta + (\rho grV^2X_\eta)_\eta +$$
$$r(PY_\eta)_\xi - r(PY_\xi)_\eta - \{\{ \mu rX_\xi[U(X_\xi X_\xi - Y_\xi Y_\xi) + V(X_\eta X_\xi - Y_\xi Y_\eta)]_\eta/g\}_\eta$$
$$-\{\{ 2\mu rY_\xi[2 (UX_\xi Y_\xi + VX_\eta Y_\xi)_\eta + (VrY_\eta X_\xi + UrY_\xi X_\xi)_\eta/r] /(3g) \}_\eta\}/ (Re_\infty)=0 \tag{1b}$$

Y Momentum Equation:

$$[\rho gr(VY_\eta + UY_\xi)]_\tau + (\rho grU^2Y_\xi)_\xi + (\rho grUVY_\eta)_\xi + (\rho grUVY_\xi)_\eta + (\rho grV^2Y_\eta)_\eta$$
$$-r(PX_\eta)_\xi + r(PX_\xi)_\eta - \{\{ \mu rY_\xi[U(Y_\xi Y_\xi - X_\xi X_\xi) + V(Y_\eta Y_\xi - X_\xi X_\eta)]_\eta/g\}_\eta - r\{ 2\mu X_\xi$$
$$[3(UY_\xi X_\xi + VY_\eta X_\xi)_\eta - (VrX_\xi Y_\eta + UrX_\xi Y_\xi)_\eta/r + (UY_\xi X_\xi + VX_\eta Y_\xi)_\eta]/(3g)\}_\eta/(Re_\infty) -$$
$$\{r\mu Y_\xi[U(Y_\xi Y_\xi - X_\xi X_\xi) + V(Y_\xi Y_\eta - X_\eta X_\xi)]_\eta /(g) \}_\eta /(Re_\infty)=0 \tag{1c}$$

Energy Equation:

$$(\rho grH)_\tau + (\rho grHU)_\xi + (\rho grHV)_\eta = \{r(\gamma-1)M_\infty^2 / [1+.5(\gamma-1)M_\infty^2]\}(Pg)_\tau -$$
$$\{[\mu rY_\xi(HY_\xi)_\eta/g]_\eta + [\mu rX_\xi(HX_\xi)_\eta/g]_\eta\}/(Re_\infty Pr) \tag{1d}$$

Equation of State:

$$P + (\gamma-1)\rho V^2/(2\gamma) = (\gamma-1)[\ 1/((\gamma-1)M_\infty^2)) + .5\ ]\ (\rho H/\gamma) \qquad (1e)$$

U and V are the contravariant velocity components in the ξ and η directions, respectively; ρ is the density; P is the pressure; H is the total enthalpy; μ is the coefficient of viscosity; γ is the ratio of specific heats; Re_∞ is the reynolds number; Pr is prandtl number and M_∞ is the free stream mach number. The quantities X_ξ, X_η, Y_ξ, Y_η are metrics associated with the coordinate transformation; r is the radial location. Two dimensional flow equations are recovered by setting r to one in (1a-e); g is the transformation jacobian and τ is time. For viscous flow computations, the X and Y momentum equations are appropriately combined to obtain the momentum balance in the ξ and η directions. Viscous diffusion terms are retained in the ξ momentum equation; all viscous dissipation terms in the η momentum and energy equations are neglected.

In the equations (1a-e), all distances have been normalized with respect to the inlet throat radius; the velocities, density, temperature, total enthalpy, viscosity are non-dimensionalized with respect to the corresponding freestream values; the pressure is non-dimensionalized with respect to twice the free stream dynamic pressure.

INITIAL AND BOUNDARY CONDITIONS

For viscous flow computations, the inviscid values are prescribed for the initial guess. Boundary conditions are such that, at the inflow U, V, ρ, P and H are all prescribed. At the outflow, for boundaries outside of the inlet and far from regions of reversed flow, the negative eigenvalue fluxes are neglected. For internal flow boundaries, the back pressure is specified. This is consistent with the operational or experimental conditions of the inlet. Far from the surface of the cowling, uniform flow conditions are imposed. At the surface, for inviscid flow calculations, zero normal velocity or injection is specified. For viscous flow computations, additional no slip and adiabatic wall temperature conditions have been prescribed for most computations. However, cold wall temperature conditions have also been considered in some calculations. A wall pressure condition is not required. The surface pressure is computed as part of the solution. For external outer boundaries, the free stream pressure is specified. More details on boundary conditions as applied to internal flows are available in reference (1,2,3,18).

DISCRETIZATION

The RNS equations are discretized based on a pressure flux-split technique. The differencing has been described in previous references (1-4) and is only briefly reviewed here. All convective or ξ derivatives are upwind or flux vector differenced. The η derivatives in the continuity and η momentum equations are mid point trapezoidal or two-point (central) differenced, whereas, the η derivatives in the ξ momentum and energy equations are three point central differenced. The three point η differencing in the ξ momentum and energy equations works quite well for normal shocks, but leads to oscillations ahead of strong oblique shocks. These oscillations are eliminated with mid-point differencing, similar to that used for the continuity and η momentum equations. For compression regions the ξ momentum equation, written at an appropriate half point is employed. For expansion regions,

the original central differencing scheme is retained. The details of this analysis are given in reference (1).

The streamwise pressure gradient is flux-split (4). This splitting is consistent with the flow physics and does not involve any discontinuous switching across shocks or contact discontinuities. The pressure gradient is given by

$$P_\xi = (\omega_{i-1/2})(P_i - P_{i-1})/\Delta\xi_i + (1 - \omega_{i+1/2})(P_{i+1} - P_i)/\Delta\xi_{i+1}$$

The parameter ω is computed as follows. For unsteady flows, where a differential form of the energy equation is employed, see reference (4), the cartesian form of ω is

$$\omega = M_\xi^2 \quad \text{for } M_\xi < 1. \text{ and } \omega = 1. \quad \text{for } M_\xi > 1.$$

For curvilinear co-ordinates the eigenvalue analysis indicates that the parameter ω should be redefined as follows (for details see reference 3)

$$\omega = M_\xi^2 . g^2/(Y_\eta^2 + X_\eta^2) \text{ for } M_\xi < 1. \text{ and } \omega = 1 \text{ for } M_\xi > 1.$$

Where Y_η, X_η and g are the metric quantities described previously in section 2.

The flux form of the streamwise pressure gradient term, with ω given at the half point is second-order accurate, see reference (4), and captures very sharp normal shocks, e.g. over three grid points. It should be noted that the flux splitting is employed only in the main flow or ξ direction. In the normal, and/or secondary flow direction, as described previously, central two or three-point differencing is applied. This discretization is capable of capturing very strong normal shocks. However, a complete flux-split formulation in both co-ordinate directions is required when considering very strong oblique shock waves, e.g., hypersonic free streams. It must be noted that, though the convective streamwise derivatives are approximated using first-order differencing the accuracy of the overall scheme is somewhere between first and second-order for RNS solutions. This analysis has previously been discussed in references (5,8). In reversed flow regions, the streamwise convection terms in the ξ momentum and energy equation are flux vector or upwind differenced and this requires that the parameter ω be set to zero, see references (2,3,4,11,14). An alternate form of flux-splitting in both ξ and η directions is currently being examined.

In subsonic attached flow regions, upstream influence is transmitted through the negative eigenvalue flux or forward differenced part of P_ξ. At the leading edge, upstream influences originate from both the upper and lower surfaces of the cowling. This is modelled as an averaged form of the ξ momentum equation, written at two half points. The details of this procedure are discussed in reference (3).

Turbulence Model

For turbulent flow computations the Baldwin-Lomax (B-L) model (19) is used. This is an algebraic, two layer eddy viscosity model. The inner model is based on the Prandtl-Van Driest formulation and the outer model is based on a modified clauser formulation. The distribution of vorticity is used to determine the length scales so that the necessity for finding the outer edge of the boundary layer is removed. Details of this model are discussed in references (19,20). It is known that for highly curved geometries or large regions of recirculation of the B-L model is inadequate. For the present study these effects are generally not dominant.

SOLUTION PROCEDURE

The discretized equations are quasilinearized and written in a nine point star in delta form.

$$A_{ij}\delta\phi_{ij-1} + B_{ij}\delta\phi_{ij} + C_{ij}\delta\phi_{ij+1} + D_{ij}\delta\phi_{i-1j} + E_{ij}\delta\phi_{i+1j} + AM_{ij}\delta\phi_{i-1j-1} + CM_{ij}\delta\phi_{i-1j+1} + EM_{ij}\delta\phi_{i+1j-1} + EP_{ij}\delta\phi_{i+1j+1} = G_{ij} \quad (2)$$

where $\delta\phi$ is the solution vector, the coefficients A_{ij} ... EM_{ij} are (5x5) matrices and G_{ij} is a (5x1) vector .

For supersonic regions where there is no upstream influence, E_{ij}, EM_{ij} and EP_{ij} are zero and the method reduces to a standard initial value problem. This system can then be easily solved using a marching technique such as line relaxation. However, for subsonic flow fields and fine meshes the convergence rates of such iterative techniques are generally significantly reduced. Moreover, for unsteady flows the physical time step limitation can also be severe (13). Iterative schemes for strongly interacting flows are also susceptible to false transients that further reduce time step requirements. Most of the difficulties that are associated with iterative or approximate factorization techniques can be overcome by the use of a direct solver. In the present study the choice of direct solver is dictated by considerations of stability, robustness and time consistency.

The Yale Sparse Matrix Package (YSMP), developed by Eisenstadt (14), and modified for coupled systems [15] and for the boundary conditions detailed previously, is applied here. This is an efficient solver as it stores only non-zero elements, and reorders the matrix using a minimum degree algorithm to minimize fill-in during the LU decomposition. However, for fine meshes and large numbers of mesh points, the memory requirement for the direct solver can become significant. Although memory associated with present day computers has constantly been increasing, access is still limited. To overcome this limitation, a domain decomposition strategy is employed. The computational domain is appropriately split into subdomains with suitable overlap between adjacent regions. Since we are dealing with flow fields that involve moving shocks, the overlap has to be sufficiently broad to accomodate the complete shock. Since captured shocks are spread over three to four grid points, an overlap of five points is specified. For further details see reference (2).

RESULTS

In the first part of the present investigation a two dimensional inlet (flat plate diffuser) is considered. The present authors have previously investigated inviscid and viscous laminar flow (Re# 12000) for this geometry, see references (1,2). Rather interesting flow physics is highlighted even by this simple geometry. Flow behaviour within a more complex geometry, axisymmetric inlet with a centerbody and cowling was also investigated. The results of this analysis are discussed in reference (3). Most results are for $M_\infty = 2.5$. Higher Mach numbers were considered and these results are presented in reference [2].

The unstart and restart of a two dimensional inlet are investigated herein.

Supersonic flow between two parallel plates with a sufficiently high back pressure is computed. Computations were performed on a 57 x 154 grid (ΔX= 0.024, ΔY_{min}= 0.00003). In the normal direction, 97 points are placed inside the diffuser and the remainder are appropriately distributed outside. The internal flow field (between the center-line and cowling) and the external flow field, are computed simultaneously. For this grid, the CPU time per iteration on the Cray Y-MP8 is about 35 seconds per iteration. The memory requirement for the above grid using domain decomposition strategy (5 domains each of approximately 15 x 154) is a little over three megawords.

In the present investigation, unstart and restart are investigated by changing the back pressure. At unstart a bow shock stands ahead of the inlet (fig.1a-b). An

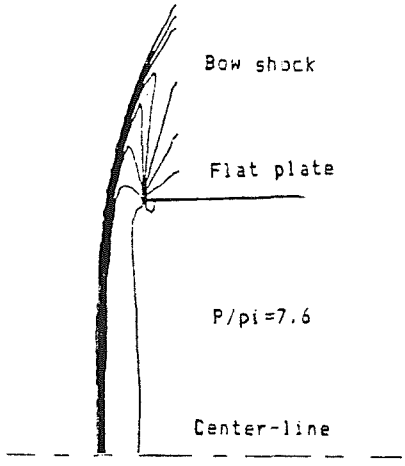

Fig.1a Unstarted Inlet

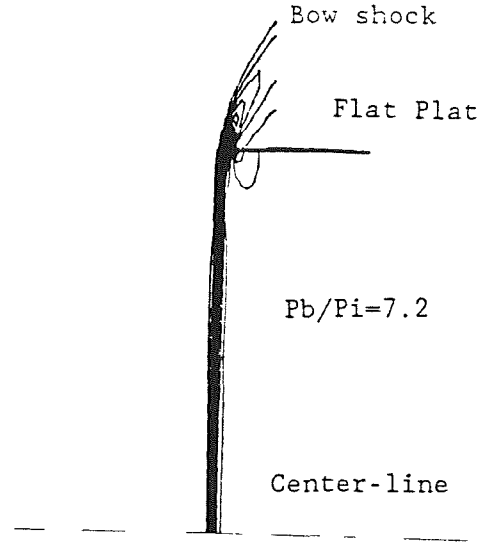

Fig.1b Unstarted Inlet

inviscid solution, for an unstarted inlet, as described in reference (1), was used as an initial solution to compute the viscous flow. Steady viscous turbulent flow (Re# 1000000) solutions for an unstarted inlet were then obtained. Convergence at each time step requires approximately 3 to 5 iterations or 150 CPU seconds. The steady state viscous results requires 25 time steps. The unstarted inlet (back pressure ratio Pb/Pi=7.2) was restarted by decreasing the back pressure ratio to 6. This is well below the critical value. Figures 2a-b depict the time history of the

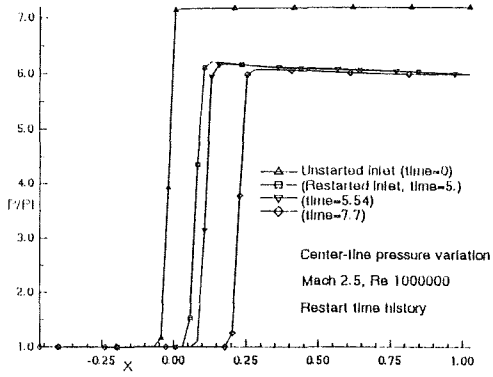

Fig.2a Time History of Unstart (Centerline Pressure)

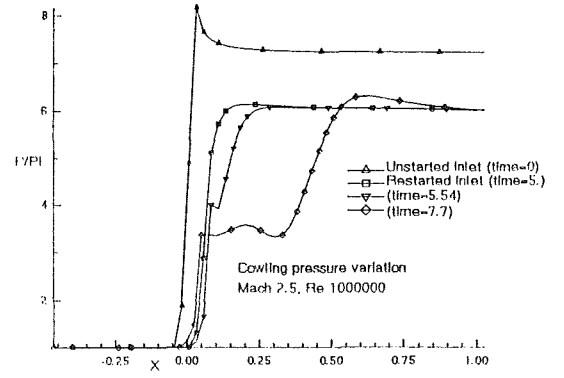

Fig.2b Time History of Unstart (Cowling Pressure)

restart process. Once the shock is swallowed the adverse pressure gradient associated with the shock generates a reversed flow region at the cowling surface. Since the shock location varies with time, the separation region is also in constant flux. A steady state is never achieved.

At a non-dimensionalized time τ of 5.0 where $\tau = \frac{tU_\infty}{L}$ and L is the throat half-width, the normal shock is swallowed (inlet restart) and lies very close to the inlet tip. At this location the terminal normal shock merges with the inlet leading edge oblique shock. The cowling pressure distribution (fig.2b) indicates a single shock close to the inlet lip. However, at time 5.54 the pressure distribution (fig.2b) indicates a double shock. Due to the separation, the boundary layer thickens considerably and this generates a strong leading edge oblique shock. At time 7.7 the pressure contours (fig.3a) indicate a very complex shock structure close to the surface. An oblique shock originates from the leading edge of the cowling lip and this shock intersects the triple point associated with the normal shock. The velocity vectors (fig.3b) depict the recirculation zone associated with the triple point shock.

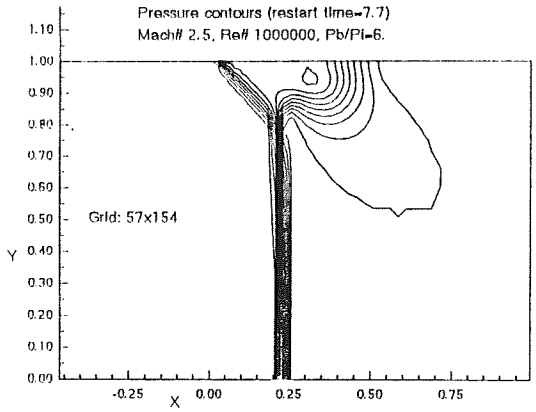

Fig.3a Shock Boundary Layer Interaction (pressure contours)

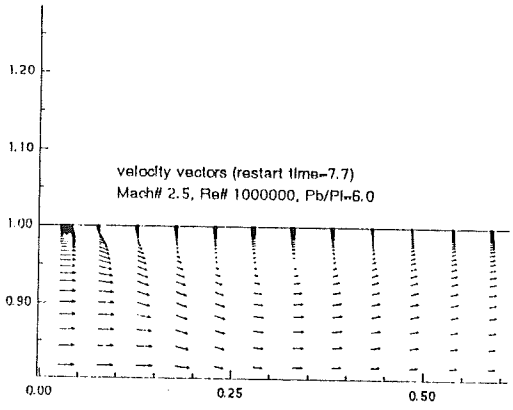

Fig.3b Velocity Vectors

Unstart of the inlet was then obtained by gradually increasing the back pressure from 6. to 7.2. As a first step, a restarted inlet with the swallowed shock very close to the cowling lip was considered. Laminar flow at a Reynolds number of 12000 was first investigated. Figures 4a-b depict the time history leading to unstart.

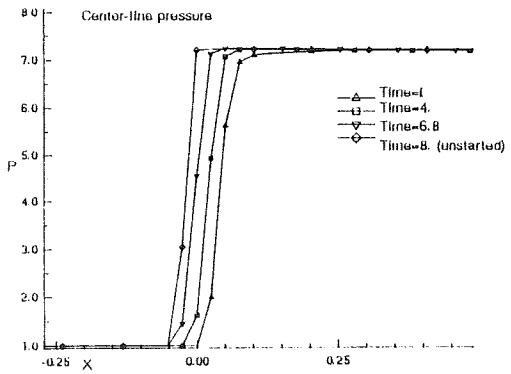

Fig.4a Time History of Unstart (mach# 2.5, Re# 12000)

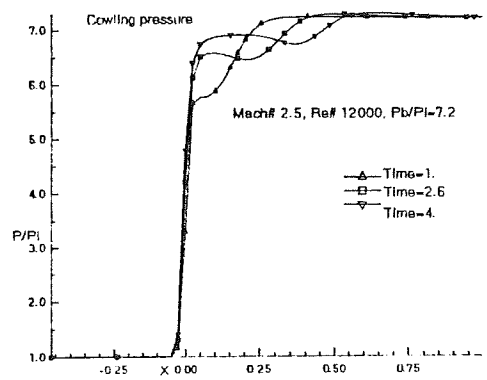

Fig.4b Time History of Unstart

Time history is recorded from the time instant (t=0) at which the back pressure is held constant at Pb/Pi=7.2. Figures 4c-d indicate that the pressure along the cowling at the shock gradually rises and a pressure pulse travels within the boundary layer towards the inlet exit. This pressure pulse is associated with a shed vortex. The skin friction, figs. 4c-d, and the velocity vector plots (figs. 5a-b)

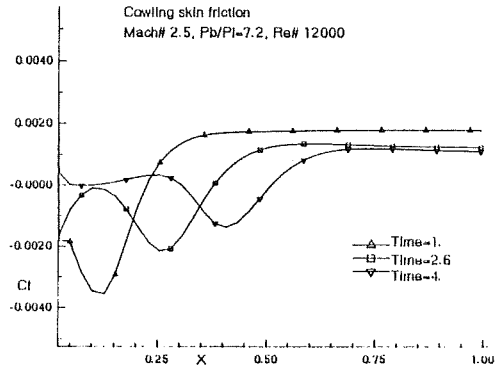

Fig.4c Skin Friction

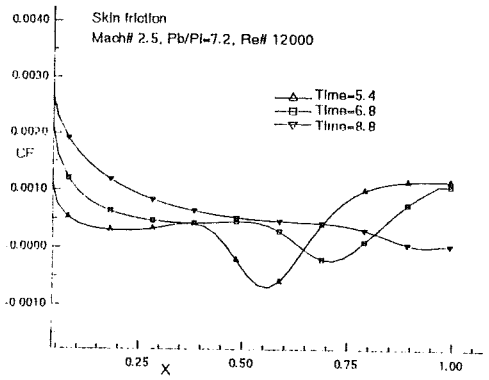

Fig.4d Skin Friction

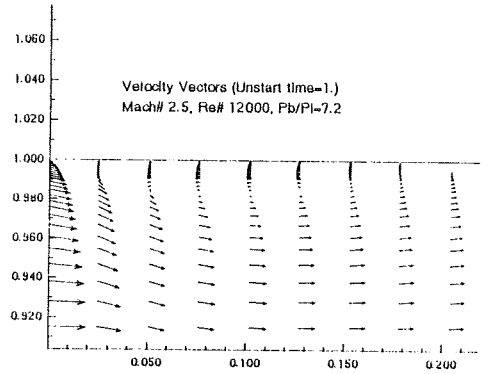

Fig.5a Velocity Vectors

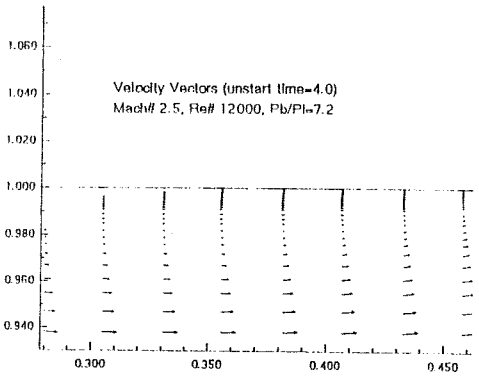

Fig.5b Velocity Vectors

depict the recirculation region associated with the moving vortex. The vortex diminishes in size and strength as it moves towards the inlet exit. These results indicate that during unstart as the shock moves towards the cowling lip, vorticity is shed and then convected downstream with the flow until it is dissipated within the boundary-layer. The resulting flow phenomena associated with unstart is therefore quite complex as it involves moving shocks and recirculation regions as well as vortex shedding and associated viscous-inviscid interactions. Current investigations include the effect of surface bleed to reduce the severity of vortex interaction.

The effects of the turbulence model was then considered. Unstart flow conditions obtained for a Reynolds number of 1000000 were investigated. The time history leading from start to unstart is depicted in Figures 6a-b. A comparison of Figure 2b (restart) and Figure 6a (unstart) indicate that the shock speed for the unstart condition is much smaller than that for the restart condition. The skin friction (fig. 6b) indicates that as the shock moves out of the inlet, the associated

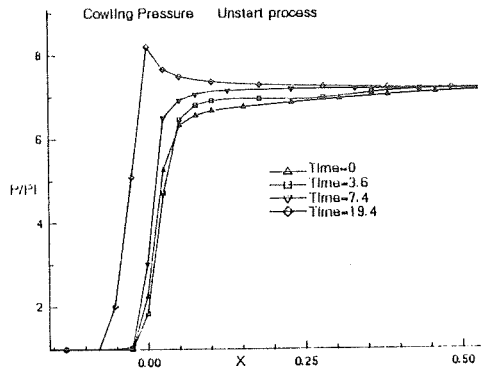

Fig.6a Time History of Unstart (mach# 2.5, Re=1000,000)

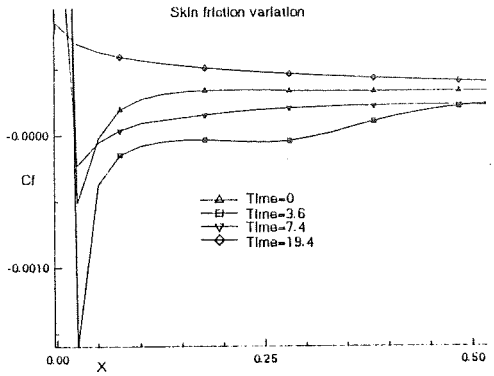

Fig.6b Skin friction

recirculation bubble diminishes in size and eventually vanishes when unstart (time=19.4) conditions are achieved. For the turbulent flow calculations, the vorticity is immediately dissipated and shedding is not observed.

For the flat plate diffuser, which represents a starting point for the simulation of transient inlet behaviour, neither computational or experimental results are available for comparison. However, there is qualitative agreement with flow visualization studies. This has been discussed in reference (2). The only detailed and quantitative assessment of accuracy is through grid refinement studies. These have previously been carried out and are discussed in reference (2). The code has also been validated for other geometries by comparing with other known solutions in reference (1).

In the second part of this study, supersonic flow in an axisymmetric inlet with a centerbody (fig.7) is investigated. In this study, the inviscid flow solution has been obtained. Computations were performed on an 89 x 115 grid. For supersonic inflow, a conical shock is formed at the tip of the centerbody. A second shock originates from the tip of the cowling and lies within the inlet (fig. 8). This

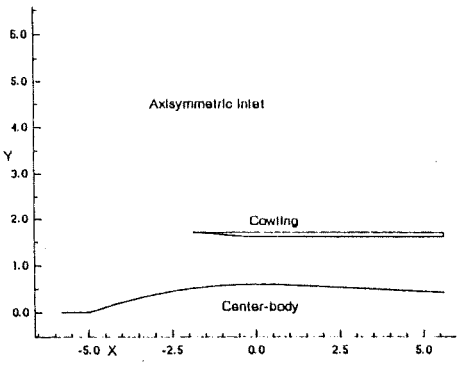

Fig.7 Axisymmetric Inlet

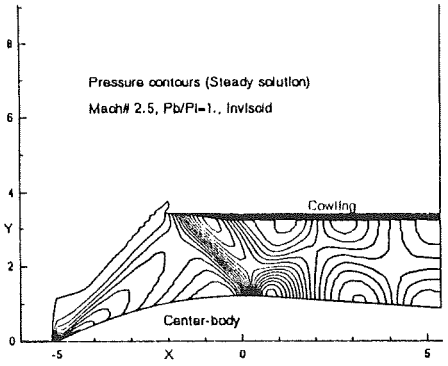

Fig.8 Pressure Contours

represents the design case and there is no mass spillage. If the back pressure at the inlet exit is raised, a terminal normal shock is formed. Figure 9a shows the pressure distribution for a back pressure to free stream pressure ratio (Pb/Pi) of

8. A terminal shock is formed and lies close to the exit (fig. 9b). If the back pressure is sufficiently high, the mass flow behind the normal shock is larger than that allowable for the given throat area. As a result, the shock moves toward the throat of the inlet and is eventually expelled from the inlet. This results in spillage of the excess mass and inlet unstart. This phenomena is further investigated herein.

A sufficiently large back pressure is applied; i.e., (Pb/Pi) = 9. The time history leading to unstart is depicted in figures 9a-b. The pressure contours (figs

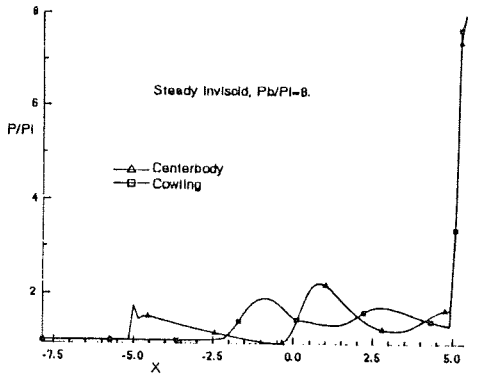

Fig.9a Pressure Distribution

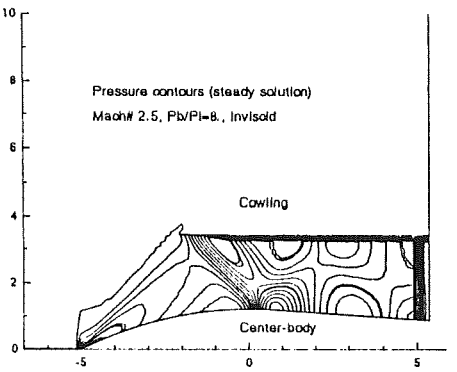

Fig.9b Pressure Contours

10a-d) depict the complex shock pattern that exists at various time intervals during unstart. At a non-dimensional time of 208., the terminal normal shock interacts with the cowling conical shock (fig. 10c). At a time of 259, the shock is expelled (fig. 10d) and the inlet unstarts. The expelled shock interacts with the centerbody conical shock and this results in a bow shock ahead of the inlet (fig.10d). The surface pressure distribution at various times is shown in figures 11a-b (fig.10). Viscous computations for this geometry are under investigation and these results will be reported in a subsequent paper.

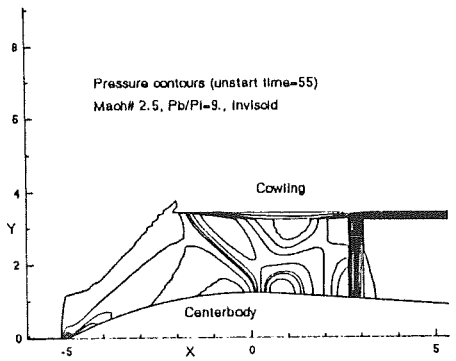

Fig.10a Pressure Contours

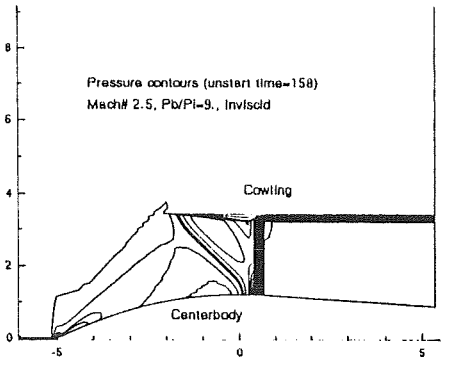

Fig.10b Pressure Contours

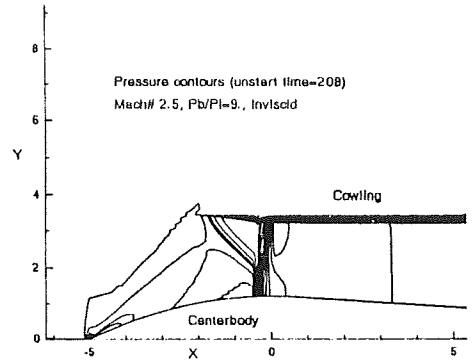

Fig.10c Pressure Contours

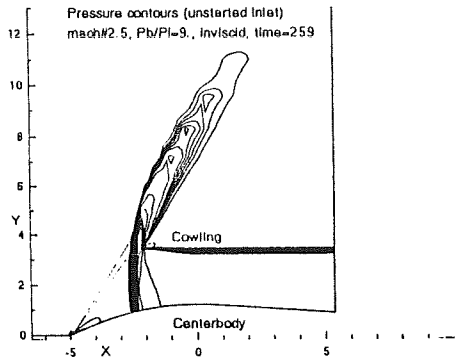

Fig.10d Pressure Contours

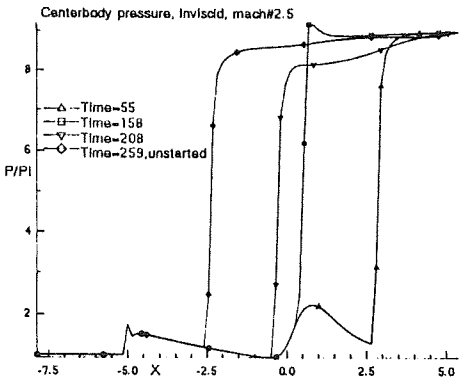

Fig.11a Centerbody Pressure Variation

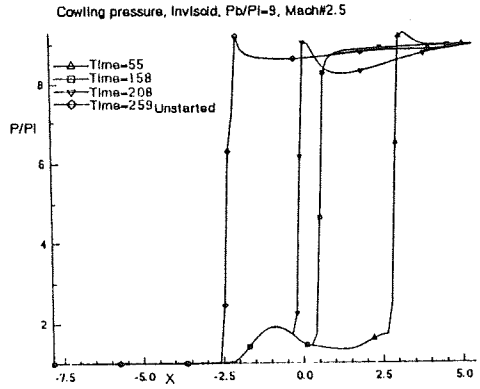

Fig.11b Cowling Pressure Variation

SUMMARY

A RNS flux-split computational procedure has been applied to investigate unstart/restart of aircraft engine inlets. A two-dimensional flat plate diffuser and an axisymmetric inlet with a centerbody has been considered. A sparse matrix direct solver combined with a domain decomposition strategy has been used to efficiently compute the complete transient flow behavior for a variety of back pressure ratios.

Unstart and/or restart of the inlet was initiated by changing the back pressure. The associated transients were efficiently captured. The applicability of the RNS flux-split procedure for unsteady flows involving moving shocks, time varying recirculation regions and shed vorticity has been demonstrated.

ACKNOWLEDGEMENT

The work has been supported in part by the NASA Lewis Research Center (T.Benson, Technical Monitor) under Grant No. NAG 3-716 and in part by the AFOSR (L. Sakell, Technical Monitor) under Contract No. F49620-85-C-0027.

The computations have been performed on the Cray Y-MP at the Ohio Supercomputer Center.

REFERENCES

1. Pordal, H.S., Khosla, P.K. and Rubin, S.G. Flux-Split Solution Procedure for the Euler Equations, International Conference on Compuatational Techniques and Applications, Brisbane, Australia, 1989.
2. Pordal, H.S., Khosla, P.K. and Rubin, S.G. A Flux-Split Solution Procedure for Unsteady Flow Calculations, To be Presented at the International Symposium on Nonsteady Fluid Dynamics, Toronto, Canada, 1990.
3. Pordal, H.S., Khosla, P.K. and Rubin, S.G. A Flux-Split Solution Procedure for Unsteady Inlet Flows, 28th Aerospace Sciences Meeting, AIAA 90-0585, Reno, Nevada, 1990.
4. Rubin, S.G, Reduced Navier Stokes/Euler Pressure Relaxation and Flux Vector Splitting, Computers and Fluids, Vol. 16, No. 4, pp. 285-290, 1988.
5. Rubin, S.G. and Reddy, D.R., Analysis of Global Pressure Relaxation for Flows with Strong Interaction and Separation, Computers and Fluids, Vol.11, No.4, pp. 281-306, 1986.
6. Khosla, P.K., and Lai, H.T., Global PNS Solutions for Subsonic Strong Interaction Flow Over a Cone-Cylinder Boat-Tail Configuration, Computers and Fluids, Vol. 11, No. 4, pp. 325-339, 1983.
7. Rubin, S.G., A Review of Marching Procedures for PNS Equations, Proceedings of a Symposium on Numerical and Physical Aspects of Aerodynamic Flows, Springer-Verlag, CA, pp. 171-186, 1982.
8. Rubin, S.G. and Reddy, D.R., Global PNS Solution for Laminar and Turbulent Flows, 6th Computational Fluid Dynamics Conference, AIAA 83-1911, Denver, MA, 1983.
9. Khosla, P.K. and Lai, H.T., Global Relaxation Procedure for Compressible Solutions of the Steady-State Euler Equations, Computers and Fluids, Vol.15, No. 2, pp. 215-218, 1987.
10. Ramakrishnan, S.V. and Rubin, S.G., Global Pressure Relaxation for Steady, Compressible, Laminar, Two Dimensional Flows with Full Pressure Coupling and Shock Waves., Report AFL 84-100, University of Cincinnati, 1984.
11. Himansu, A., Khosla, P.K. and Rubin, S.G., Three Dimensional Recirculating Flows, 27th Aerospace Sciences Meeting, AIAA 89-0552, Reno, Nevada, 1989.
12. Ramakrishnan, S.V. and Rubin, S.G., Numerical Solution of Unsteady Compressible Reduced Navier Stokes Equations, 24th Aerospace Sciences Meeting, AIAA 86-0205, Reno, Nevada, 1986.
13. Ramakrishnan, S.V. and Rubin, S.G., Time Consistent Pressure Relaxation Procedure for Compressible Reduced Navier Stokes Equations, AIAA Journal, Vol. 25, No. 7, pp. 905-913, 1987.
14. Rubin, S.G. and Himansu, A., Convergence Properties of High Reynolds Number Separated Flow, Accepted for publication, International Journal for Numerical Methods in Fluids, 1989.
15. Bender, E.E., The use of Direct Sparse Matrix Solver and Newton Iteration for the Numerical Solution of Fluid Flow, Ph'd thesis, University of Cincinnati, 1988.
16. Eisenstadt, S.G., Gursky, M.C., Schultz, M.H. and Sherman, A.H., Yale Sparse Matrix Package II. The Non-Symmetric Codes, Report 114, Yale University Department of Computer Science, 1977.
17. Khosla, P.K. and Rubin, S.G., Consistent Strongly Implicit Iterative Procedure for Two Dimensional Unsteady and Three Dimensional Space-Marching Flow Calculations, Computers and Fluids, Vol. 15, No. 4, pp. 361-377, 1987.

18. Reddy, D.R.,and Rubin, S.G., Consistent Boundary Condition for Reduced Navier Stokes Scheme Applied to Three Dimensional Internal Viscous Flows, 26th Aerospace Sciences Meeting, AIAA 88-0714, Reno, Nevada, 1988.
19. Baldwin, B.S. and Lomax, H., Thin Layer Approximation and Algebraic Model for Separated Turbulent Flows, 16th Aerospace Sciences Meeting, AIAA 78-257, Huntsville, Alabama, 1978.
20. Visbal, M. and Knight, D., The Baldwin-Lomax Turbulence Model for Two-Dimensional Shock-Wave Boundary-Layer Interactions, AIAA Journal, Vol. 22, No.7, pp. 921-927, July, 1984.